Hindawi
Mathematical Problems in Engineering
Volume 2018, Article ID 6250158, 9 pages
https://doi.org/10.1155/2018/6250158

Research Article

Seabed Dynamic Response of Offshore Wind Turbine Foundation under Vertical Harmonic Loading: An Analytic Solution

Dimitrios G. Pavlou and Yuzhu Li

Department of Mechanical and Structural Engineering and Materials Science, University of Stavanger, 4036 Stavanger, Norway

Correspondence should be addressed to Dimitrios G. Pavlou; dimitrios.g.pavlou@uis.no

Received 6 September 2018; Accepted 15 October 2018; Published 25 October 2018

Academic Editor: José A. Correia

Wave-induced dynamic loads yield displacement and stress propagation on the seabed beneath the offshore wind turbine foundation. Existing attempts to calculate the displacement/stress propagation based on commercial software packages or numerical solvers usually ignore the inertial effects and provide quasi-static solution for the dynamic problem or ignore the damping effect of the soil. Since real time displacement measurements on the seabed are difficult to be carried out, the existing results are not able to be validated and the conclusions are rather arbitrary. Analytic solutions can provide accurate results and are less time-consuming and more computationally efficient than the numerical approaches but difficult to be achieved. In the present study an exact solution of the wave propagation in the seabed under harmonic excitation of the wind turbine foundation is achieved. The solution is based on integral transforms and stress functions. Verification of the solution is provided and a representative example is solved and commended.

1. Introduction

Existing attempts to calculate the displacement and stress propagation on the seabed beneath the offshore wind turbine foundation are mainly based on commercial software packages or numerical solvers [1–4]. In the most existing works, the solutions to the wave, structure, and seabed interaction problems are based on a 'one-way coupling' assumption (e.g., [1, 3, 4]). In [3–5], the Biot's equation [6, 7] is adopted to model the soil behaviour. The inertial effects are ignored, yielding quasi-static solution for the dynamic displacement propagation in the soil. Moreover, the assumption of the elastic behaviour of the soil does not take into account the damping effect. Since real-time displacement measurements on the seabed beneath the foundation are difficult to be carried out, the existing numerical results and the conclusions are not validated. Also, the usage of the numerical tools can have a high computational cost and is time-consuming for solving the coupling problem in order to achieve a low residual.

Analytic solutions to such problems are more accurate and more efficient compared to the numerical ways but are difficult to achieve. A fundamental contact mechanics solution based on Green's functions and boundary integral equation solution has been achieved in [8] for the stress analysis of the soil-foundation interaction under static torsion. Analytical solutions for dissimilar or homogeneous elastic medium (space and half-space) containing interfacial cracks, under axial, radial, and torsional loading sources are provided in [9–16]. Using double integral transforms, the dual integral equations for wave propagation of a cracked medium under transient dynamic loading are originally solved in [17]. Analytical solutions for the dynamic response of foundation on elastic and viscoelastic soil are achieved in [18–20]. Interaction of foundation piles embedded in transversely isotropic soil under dynamic loading is analysed in [21, 22]. Structural analysis of wind turbine tower under environmental loads is performed in [23], and analytical solution for evaluating the dynamic response of plates under underwater transient loads is presented in [24].

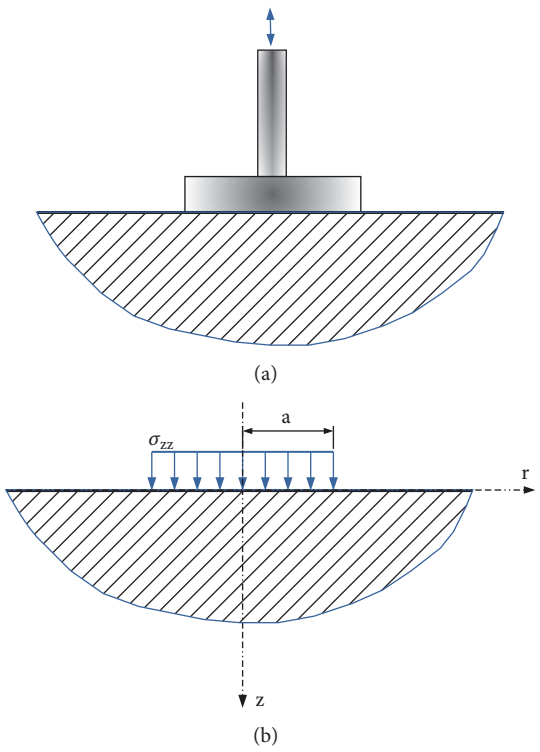

Figure 1: Circular foundation on elastic seabed: (a) physical model and (b) mechanical model.

In the present study, an exact solution of the wave propagation in the seabed under vertical harmonic excitation of the wind turbine foundation is achieved. The solution is based on integral transforms and stress functions. A representative example is solved and commended in the present work. Verification of the solution is provided by solving a specific case of a sudden point load on the solid surface and the solution is verified against the existing solution in [25]. The proposed solution has two benefits: (a) it takes into account the inertial effects in the displacement propagation, and (b) the solution is analytic, yielding better accuracy and negligible computation cost. The limitation of the present version is that it does not include the effect of porous material and damping yet. The analytic solution in the present work can be extended for solving porous media with time-varying dynamic loads taking into account the material damping effect.

2. Formulation of the Problem

A circular foundation based on an elastic half-space (e.g., rock seabed) is subjected to vertical harmonic load. The coordinate system of the foundation is shown in Figure 1. A pressure distribution

$$\sigma_{zz}(r,0,t) = Z\left[H\langle r\rangle - H\langle r-a\rangle\right]\sin\omega t \tag{1}$$

is assumed to act on the surface of the half-space. The symbol $H\langle r\rangle$ denotes the Heaviside function. The term $[H\langle r\rangle - H\langle r-a\rangle]$ represents the uniform pressure distribution in the area $0 \le r \le \alpha$ (Figure 1(b)), the term $\sin\omega t$ is the harmonic function of time, and Z is the amplitude of the load. The harmonic term $\sin\omega t$ causes wave propagation in the domain of the elastic seabed.

Since no body-forces exist, the governing equation in terms of displacements (Navier's equation) can be written [26] as

$$(\lambda+\mu)\nabla\nabla\bullet\vec{u} + \mu\nabla^2\vec{u} = \rho\frac{\partial^2\vec{u}}{\partial t^2} \tag{2}$$

where $\vec{u}$ is the vector of the displacement components u_r, u_z, u_ϑ in the directions r, z, ϑ respectively, λ, μ are the Lame constants, and ρ is the material density. Taking into account the axisymmetric geometry and load, the displacement component u_ϑ is zero. Therefore, the displacement vector can be expressed by the following equation:

$$\vec{u}(r,z,t) = u_r\vec{e}_r + u_z\vec{e}_z \tag{3}$$

where $\vec{e}_r, \vec{e}_z$ are the unit vectors in the directions r, z respectively. In terms of scalar and vector potentials φ, $\vec{h}$, (3) can be written [25] as

$$\vec{u} = \nabla\varphi + \nabla\times\left(h_\vartheta\vec{e}_\vartheta\right) \tag{4}$$

With the aid of (4), (2) yields

$$\nabla^2\varphi = \frac{1}{c_1^2}\frac{\partial^2\varphi}{\partial t^2} \tag{5}$$

$$\nabla^2 h_\vartheta - \frac{1}{r^2}h_\vartheta = \frac{1}{c_2^2}\frac{\partial^2 h_\vartheta}{\partial t^2} \tag{6}$$

In above equations the parameters c_1, c_2 are given in [25] by the formulae

$$c_1 = \sqrt{\frac{\lambda+2\mu}{\rho}} \tag{7}$$

$$c_2 = \sqrt{\frac{\mu}{\rho}} \tag{8}$$

and express the propagation velocity of the dilatational and rotational waves, respectively. The operator ∇^2 in polar coordinates is given by the following equation:

$$\nabla^2 = \frac{1}{r}\frac{\partial\left(r\left(\partial/\partial r\right)\right)}{\partial r} + \frac{\partial^2}{\partial z^2} \tag{9}$$

If we use [25] a function ψ, where

$$h_\vartheta = -\frac{\partial\psi}{\partial r} \tag{10}$$

(6) can further be simplified:

$$\nabla^2\psi = \frac{1}{c_2^2}\frac{\partial^2\psi}{\partial t^2} \tag{11}$$

With the aid of (4), (5), (10), and (11), the stresses (in polar coordinates) of Appendix A and the displacements can now be written in terms of the scalar functions φ, ψ.

(a) Displacements

$$u_r = \frac{\partial \varphi}{\partial r} + \frac{\partial^2 \psi}{\partial r \partial z} \tag{12}$$

$$u_\vartheta = 0 \tag{13}$$

$$u_z = \frac{\partial \varphi}{\partial z} + \frac{\partial^2 \psi}{\partial z^2} - \frac{1}{c_2^2}\frac{\partial^2 \psi}{\partial t^2} \tag{14}$$

(b) Stresses

$$\sigma_{rr} = \lambda \nabla^2 \varphi + 2\mu \left(\frac{\partial^2 \varphi}{\partial r^2} + \frac{\partial^3 \psi}{\partial r^2 \partial z} \right) \tag{15}$$

$$\sigma_{\vartheta\vartheta} = \lambda \nabla^2 \varphi + \frac{2\mu}{r} \left(\frac{\partial \varphi}{\partial r} + \frac{\partial^2 \psi}{\partial r \partial z} \right) \tag{16}$$

$$\sigma_{zz} = \lambda \nabla^2 \varphi + 2\mu \frac{\partial}{\partial z} \left(\frac{\partial \varphi}{\partial z} + \frac{\partial^2 \psi}{\partial z^2} - \frac{1}{c_2^2}\frac{\partial^2 \psi}{\partial t^2} \right) \tag{17}$$

$$\sigma_{rz} = \mu \frac{\partial}{\partial r} \left(2\frac{\partial \varphi}{\partial z} + 2\frac{\partial^2 \psi}{\partial z^2} - \frac{1}{c_2^2}\frac{\partial^2 \psi}{\partial t^2} \right) \tag{18}$$

$$\sigma_{\vartheta z} = 0 \tag{19}$$

$$\sigma_{r\vartheta} = 0 \tag{20}$$

3. Solution of the Dynamic Problem

For the solution of the problem, Laplace and Hankel integral transforms will be applied on the governing equations and boundary conditions. The definition and some important properties of the above transforms are given below.

3.1. Laplace Transform of Any Function $f(t)$

$$L\{f(t); t \longrightarrow p\} = F(p) = p\int_0^\infty f(t)\, e^{-pt} dt \tag{21}$$

The inverse form of Laplace transform is given by the following formula:

$$L^{-1}\{F(p); p \longrightarrow t\} = f(t) = \frac{1}{2\pi i}\int_{a-i\infty}^{a+i\infty} \frac{F(p)}{p} e^{tp} dp \tag{22}$$

3.2. Hankel Transform of Any Function $g(r)$

$$H_n\{g(r); r \longrightarrow \xi\} = \overline{g}(\xi) = \int_0^\infty g(r)\, r J_n(r\xi)\, dr \tag{23}$$

The inverse form of Hankel transform is given by the following formula:

$$H_n^{-1}\{\overline{g}(\xi); \xi \longrightarrow r\} = g(r) = \int_0^\infty \overline{g}(\xi)\, \xi J_n(r\xi)\, d\xi \tag{24}$$

Taking the Laplace transform of the displacement and stress components given by (12)-(20), formulae (B.1)-(B.7) in Appendix B will be obtained.

3.3. Boundary Conditions. The surface $z = 0$ of the half-space is loaded by the stress $\sigma_{zz}(r, 0, t)$ given by (1). Since the surface is free of shear stresses, the following condition is valid:

$$\sigma_{zr}(r, 0, t) = 0 \tag{25}$$

Taking into account the definition of the Hankel and inverse Hankel transform given by (23) and (24), (1) can be written in the form

$$\begin{aligned} &\sigma_{zz}(r, 0, t) \\ &\quad = ZH_0\left\{H_0^{-1}\{\sigma_{zz}(r, 0, t); r \longrightarrow \xi\}; \xi \longrightarrow r\right\} \end{aligned} \tag{26}$$

or

$$\begin{aligned} \sigma_{zz}(r, 0, t) = Z \sin \omega t \int_0^\infty \xi J_0(\xi r)\, d\xi \\ \cdot \int_0^\infty [H\langle r\rangle - H\langle r - a\rangle]\, x J_0(x\xi)\, dx \end{aligned} \tag{27}$$

With the aid of the properties [27]

$$\begin{aligned} H_0\{H\langle a - x\rangle; x \longrightarrow \xi\} &= \int_0^\infty H\langle a - x\rangle\, x J_0(x\xi)\, dx \\ &= \xi^{-1} a J_1(a\xi) \end{aligned} \tag{28}$$

$$H_0\{H\langle -x\rangle; x \longrightarrow \xi\} = 0 \tag{29}$$

(27) yields

$$\sigma_{zz}(r, 0, t) = Za \sin \omega t \int_0^\infty J_0(\xi r)\, J_1(a\xi)\, d\xi \tag{30}$$

Taking the Laplace transform of above equation, the following formula can be obtained:

$$\begin{aligned} S_{zz}(r, 0, p) &= L\{\sigma_{zz}(r, 0, t); t \longrightarrow p\} \\ &= Za\int_0^\infty \frac{\omega}{p^2 + \omega^2} J_0(\xi r)\, J_1(a\xi)\, d\xi \end{aligned} \tag{31}$$

As a consequence of the definition of the Heaviside function, the following equations can be obtained:

$$H\langle x\rangle = 1 - H\langle -x\rangle \tag{32}$$

$$H\langle x - a\rangle = 1 - H\langle a - x\rangle \tag{33}$$

Combination of (28) and (33) yields

$$\int_0^\infty H\langle x - a\rangle\, x J_0(x\xi)\, dx = 1 - \xi^{-1} a J_1(a\xi) \tag{34}$$

With the aid of (29), (32), (33), and (34), (27) can be written as

$$\sigma_{zz}(r, 0, t) = Za \sin \omega t \int_0^\infty \xi J_0(\xi r) \left[\frac{1}{\xi} J_1(a\xi)\right] d\xi \tag{35}$$

Using the notation

$$\overline{g}(\xi) = \frac{1}{\xi} J_1(a\xi) \tag{36}$$

(35) can be written:

$$\sigma_{zz}(r,0,t) = Za \sin \omega t \int_0^\infty \overline{g}(\xi)\, \xi J_0(\xi r)\, d\xi \tag{37}$$

According to (24), above equation yields

$$\sigma_{zz}(r,0,t) = Za \sin \omega t H_0^{-1} \{\overline{g}(\xi); \xi \longrightarrow r\} \tag{38}$$

Taking the Hankel transform of above equation, the following formula can be obtained:

$$\overline{\sigma}_{zz}(\xi,0,t) = Za \sin \omega t \overline{g}(\xi) \tag{39}$$

or

$$\overline{\sigma}_{zz}(\xi,0,t) = Za \sin \omega t \frac{1}{\xi} J_1(a\xi) \tag{40}$$

Then, the Laplace transform of (40) yields

$$\overline{S}_{zz}(\xi,0,p) = Za \frac{\omega}{p^2+\omega^2} \frac{1}{\xi} J_1(a\xi) \tag{41}$$

Taking the Laplace and Hankel transform to the boundary condition given by (25), the following result can be obtained:

$$\overline{T}_{zr}(\xi,0,p) = 0 \tag{42}$$

Applying the Laplace transform in (17) and (18),

$$\begin{aligned} S_{zz}(r,z,p) &= L\{\sigma_{zz}(r,z,t); t \longrightarrow p\} \\ &= \lambda \nabla^2 \Phi + 2\mu \frac{\partial}{\partial z} \left(\frac{\partial \Phi}{\partial z} + \frac{\partial^2 \Psi}{\partial z^2} - \frac{p^2}{c_2^2} \Psi \right) \end{aligned} \tag{43}$$

$$\begin{aligned} T_{rz}(r,z,p) &= L\{\tau_{rz}(r,z,t); t \longrightarrow p\} \\ &= \mu \frac{\partial}{\partial r} \left(2\frac{\partial \Phi}{\partial z} + 2\frac{\partial^2 \Psi}{\partial z^2} - \frac{p^2}{c_2^2} \Psi \right) \end{aligned} \tag{44}$$

Taking the Hankel transform $H_0\{\bullet; r \longrightarrow \xi\}$ to above equations, the following formulae can be obtained:

$$\overline{S}_{zz}(\xi,z,p) = \lambda h^2 \overline{\Phi} + 2\mu \left(\frac{\partial^2 \overline{\Phi}}{\partial z^2} + \frac{\partial^3 \overline{\Psi}}{\partial z^3} - \kappa^2 \frac{\partial \overline{\Psi}}{\partial z} \right) \tag{45}$$

$$\overline{T}_{rz}(\xi,z,p) = -\mu\xi \left(2\frac{\partial \overline{\Phi}}{\partial z} + 2\frac{\partial^2 \overline{\Psi}}{\partial z^2} - \kappa^2 \overline{\Psi} \right) \tag{46}$$

where

$$h = \frac{p}{c_1} \tag{47}$$

$$\kappa = \frac{p}{c_2} \tag{48}$$

Combining (41) with (45) and (42) with (46), the following system in terms of $\overline{\Phi}, \overline{\Psi}$ can be obtained:

$$\begin{aligned} &\lambda h^2 \overline{\Phi} + 2\mu \left(\frac{\partial^2 \overline{\Phi}}{\partial z^2} + \frac{\partial^3 \overline{\Psi}}{\partial z^3} - \kappa^2 \frac{\partial \overline{\Psi}}{\partial z} \right) \\ &\quad = Za \frac{\omega}{p^2+\omega^2} \frac{1}{\xi} J_1(a\xi), \quad z = 0 \end{aligned} \tag{49}$$

$$-\mu\xi \left(2\frac{\partial \overline{\Phi}}{\partial z} + 2\frac{\partial^2 \overline{\Psi}}{\partial z^2} - \kappa^2 \overline{\Psi} \right) = 0, \quad z = 0 \tag{50}$$

3.4. Determination of the Functions φ, ψ. In order to solve the system of (49) and (50), Laplace and Hankel transform will be applied to the governing equations (5) and (11). The Laplace transformation of (5) and (11) yields

$$\nabla^2 \Phi - \frac{p^2}{c_1^2} \Phi = 0 \tag{51}$$

$$\nabla^2 \Psi - \frac{p^2}{c_2^2} \Psi = 0 \tag{52}$$

Taking the Hankel transform $H_0\{\bullet; r \longrightarrow \xi\}$ to above equations, the following ordinary differential equations can be obtained:

$$\frac{d^2 \overline{\Phi}}{dz^2} - \left(\xi^2 + h^2\right) \overline{\Phi} = 0 \tag{53}$$

$$\frac{d^2 \overline{\Psi}}{dz^2} - \left(\xi^2 + \kappa^2\right) \overline{\Psi} = 0 \tag{54}$$

The solution of above equations is

$$\overline{\Phi} = A_1 e^{-\alpha z} + B_1 e^{\alpha z} \tag{55}$$

$$\overline{\Psi} = A_2 e^{-\beta z} + B_2 e^{\beta z} \tag{56}$$

where

$$\alpha = \sqrt{\xi^2 + h^2} \tag{57}$$

$$\beta = \sqrt{\xi^2 + \kappa^2} \tag{58}$$

For $z \longrightarrow \infty$ the functions $\overline{\Phi}, \overline{\Psi}$ will be unbounded because of the terms $B_1 e^{\alpha z}$ and $B_2 e^{\beta z}$, respectively. Therefore, the following conditions should be valid:

$$B_1 = 0 \tag{59}$$

$$B_2 = 0 \tag{60}$$

Then,

$$\overline{\Phi} = A_1 e^{-\alpha z} \tag{61}$$

$$\overline{\Psi} = A_2 e^{-\beta z} \tag{62}$$

With the aid of above two equations, the system of (49) and (50), for $z = 0$, yields

$$\left(\lambda h^2 + 2\mu\alpha^2\right) A_1 - 2\mu\beta\left(\beta^2 - \kappa^2\right) A_2 = Za\frac{\omega}{p^2+\omega^2}\frac{1}{\xi}J_1(a\xi) \tag{63}$$

$$-2\alpha A_1 + \left(2\beta^2 - \kappa^2\right) A_2 = 0 \tag{64}$$

Combining (47) with (57) and (48) with (58), the following formulae can be obtained:

$$\lambda h^2 + 2\mu\alpha^2 = \mu\left(\kappa^2 + 2\xi^2\right) \tag{65}$$

$$\beta^2 - \kappa^2 = \xi^2 \tag{66}$$

$$2\beta^2 - \kappa^2 = 2\xi^2 + \kappa^2 \tag{67}$$

With the aid of (57)-(67), the system of algebraic equations (63) and (64) can be written as

$$\begin{bmatrix} \left(2\xi^2+\kappa^2\right) & -2\beta\xi^2 \\ -2\alpha & \left(2\xi^2+\kappa^2\right) \end{bmatrix} \begin{Bmatrix} A_1 \\ A_2 \end{Bmatrix} = \begin{Bmatrix} \frac{Za}{\mu}\frac{\omega}{p^2+\omega^2}\frac{1}{\xi}J_1(a\xi) \\ 0 \end{Bmatrix} \tag{68}$$

yielding

$$\begin{Bmatrix} A_1 \\ A_2 \end{Bmatrix} = \frac{Za}{\mu}\frac{\omega}{p^2+\omega^2}\frac{J_1(a\xi)}{D}\frac{1}{\xi}\begin{Bmatrix} 2\xi^2+\kappa^2 \\ 2\alpha \end{Bmatrix} \tag{69}$$

where

$$D = \left(2\xi^2 + \kappa^2\right) - 4\alpha\beta\xi^2 \tag{70}$$

With the aid of (69) and (70), the functions given by (61), (62) can now be obtained:

$$\begin{Bmatrix} \overline{\Phi} \\ \overline{\Psi} \end{Bmatrix} = \frac{Za}{\mu}\frac{\omega}{p^2+\omega^2}\frac{J_1(a\xi)}{D}\frac{1}{\xi}\begin{Bmatrix} \left(2\xi^2+\kappa^2\right)e^{-\alpha z} \\ 2\alpha e^{-\beta z} \end{Bmatrix} \tag{71}$$

Since all the displacement and stress components given by (12)-(20) are expressed in terms of the functions φ, ψ the inverse Hankel transform $H_0^{-1}\{\bullet; \xi \longrightarrow r\}$ of above equation yields the solution of the problem.

3.5. Inversion of the Hankel Transform. Taking the inverse Hankel transform $H_0^{-1}\{\bullet; \xi \longrightarrow r\}$ in (71), the following result can be obtained:

$$\begin{Bmatrix} \Phi \\ \Psi \end{Bmatrix} = H_0^{-1}\left\{\begin{Bmatrix} \overline{\Phi} \\ \overline{\Psi} \end{Bmatrix}; \xi \longrightarrow r\right\} = \frac{Za}{\mu}\frac{\omega}{p^2+\omega^2} \cdot \int_0^\infty \frac{J_1(a\xi)}{D}\begin{Bmatrix} \left(2\xi^2+\kappa^2\right)e^{-\alpha z} \\ 2\alpha e^{-\beta z} \end{Bmatrix} J_0(\xi r)\, d\xi \tag{72}$$

Taking into account (72), the Laplace transformed displacements given in Appendix B can now be written as

$$U_r(r,z,p) = -\frac{Za}{\mu}\frac{\omega}{p^2+\omega^2} \cdot \int_0^\infty \frac{\xi\left[\left(2\xi^2+\kappa^2\right)e^{-\alpha z} - 2\alpha\beta e^{-\beta z}\right]}{D} J_1(\xi r)\, J_1(a\xi)\, d\xi \tag{73}$$

$$U_z(r,z,p) = \frac{Za}{\mu}\frac{\omega}{p^2+\omega^2} \cdot \int_0^\infty \frac{\left[-\alpha\left(2\xi^2+\kappa^2\right)e^{-\alpha z} + 2\alpha\left(\beta^2-\kappa^2\right)e^{-\beta z}\right]}{D} J_0(\xi r) \cdot J_1(a\xi)\, d\xi \tag{74}$$

Taking the inverse Laplace transform of above equations, the final solution for the displacements $u_r(r,z,t), u_z(r,z,t)$ can be obtained:

$$u_r(r,z,t) = L^{-1}\left\{U_r(r,z,p); p \longrightarrow t\right\} \tag{75}$$

$$u_z(r,z,t) = L^{-1}\left\{U_z(r,z,p); p \longrightarrow t\right\} \tag{76}$$

Above inverse Laplace transforms can be carried out numerically with the aid of the Stehfest [28] method.

4. Numerical Example and Verification of the Solution

4.1. Numerical Example. The derived solution given by (75) and (76) can now be implemented to a representative example. The dynamic load is a uniform pressure acting on a circular surface with radius a. The load can be modeled by a harmonic function and can be represented in terms of the variables r, t by (1). The selected data for the proposed loading function are $Z = 1.0\,N$, $a = 8.2\,m$, $\omega = 0.94\,rad/s$, and the material properties for the soil are $c_1 = 355\,m/s$, $c_2 = 309\,m/s$, $\mu = 2.137 \times 10^8\,N/m^2$. For the inverse Laplace transforms of (75) and (76), the Stehfest [28] method is adopted. According to this method, the functions $u_r(r,z,t), u_z(r,z,t)$ can be obtained by the following formula:

$$\begin{Bmatrix} u_r(r,z,t) \\ u_z(r,z,t) \end{Bmatrix} \approx \frac{\ln 2}{t}\sum_{n=1}^{N} c_n \begin{Bmatrix} U_r\left(r,z,\frac{n\ln 2}{t}\right) \\ U_z\left(r,z,\frac{n\ln 2}{t}\right) \end{Bmatrix} \tag{77}$$

where

$$c_n = (-1)^{n+N/2} \cdot \sum_{k=(n+1)/2}^{\min\{n,N/2\}} \frac{k^{N/2}(2k)!}{(N/2-k)!k!(k-1)!(n-k)!(2k-n)!} \tag{78}$$

In above equation, N is a free even number representing the number of terms used in the summation. Values within the range $10 \le N \le 24$ yield sufficient accuracy (e.g., [29]). In the present study we adopted the value N=24.

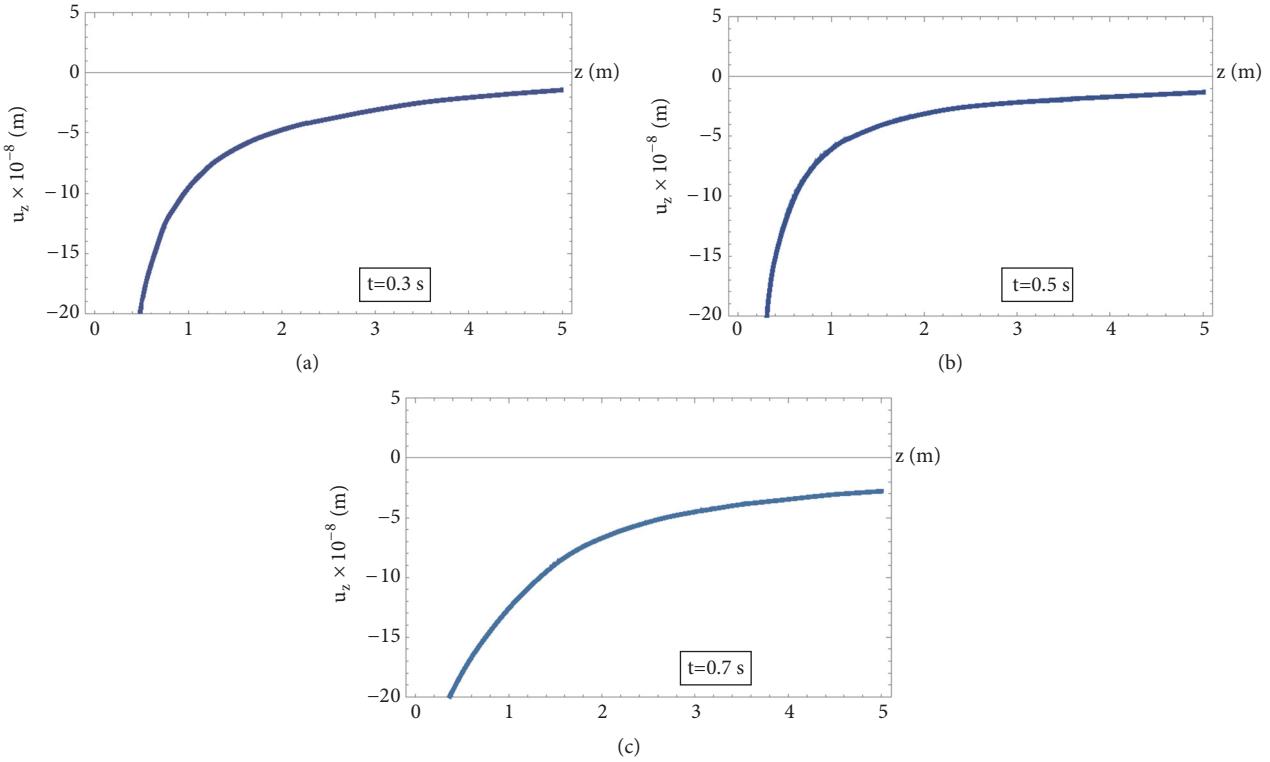

FIGURE 2: Displacement distribution u_z versus z for $r = 0$ and $t = 0.3, 0.5, 0.7\ s$.

For $r = 0$, the Bessel function $J_1(\xi r)$ is null. Therefore, (73) yields $U_r = 0$. With the aid of the standard software "Mathematica" [30] the displacement distribution u_z versus z for $r = 0$ and $t = 0.3, 0.5, 0.7\ s$ is demonstrated in Figures 2(a), 2(b), and 2(c).

According to these findings, the displacement tends to reach the z-axis asymptotically due to the terms e^{-az} and $e^{-\beta z}$ in (74).

4.2. Verification of the Solution. The derived solution can be adjusted to provide the surface displacement distribution for the specific case of a suddenly applied point load given by the following equation:

$$q(r, 0, t) = P\frac{\delta(r)}{2\pi r}H\langle t\rangle \tag{79}$$

where $\delta(r)$ is the Dirac Delta function of the variable r and $H\langle t\rangle$ is the Heaviside step function of time t. Solution for this specific case is available in [25]:

$$U_r(r, z, p) = \frac{P}{2\pi\mu p} \cdot \int_0^\infty \frac{\xi^2\left[\left(2\xi^2 + \kappa^2\right)e^{-\alpha z} - 2\alpha\beta e^{-\beta z}\right]}{D} J_1(\xi r)\, d\xi \tag{80}$$

$$U_z(r, z, p) = \frac{P}{2\pi\mu p} \cdot \int_0^\infty \frac{\left[-\alpha\xi\left(2\xi^2 + \kappa^2\right)e^{-\alpha z} + 2\alpha\xi^3 e^{-\beta z}\right]}{D} J_0(\xi r)\, d\xi \tag{81}$$

Following the procedure of [14], the point load P is given by the following equation:

$$P = Z\pi a^2 \tag{82}$$

Therefore,

$$Z = \frac{P}{\pi a^2} \tag{83}$$

The above term for the uniform distributed load Z should be placed in (73) and (74). On the other hand, the Laplace transform

$$\frac{\omega}{\omega^2 + p^2} = L\{\sin\omega t; t \longrightarrow p\} \tag{84}$$

should be replaced in (73) and (74) by the Laplace transform:

$$\frac{1}{p} = L\{H\langle t\rangle; t \longrightarrow p\} \tag{85}$$

For the case of point load P, the radius a of the circular surface of the equivalent uniform load Z given by (83) is $a \longrightarrow 0$. Therefore, (73) and (74) yield

$$U_r(r, z, p) = \lim_{a\longrightarrow 0}\left\{-\frac{\left(P/\pi a^2\right)a}{\mu}\frac{1}{p} \cdot \int_0^\infty \frac{\xi\left[\left(2\xi^2 + \kappa^2\right)e^{-\alpha z} - 2\alpha\beta e^{-\beta z}\right]}{D} J_1(\xi r) \cdot J_1(a\xi)\, d\xi\right\} \tag{86}$$

$$U_z(r,z,p) = \lim_{a\longrightarrow 0}\left\{\frac{\left(P/\pi a^2\right)a}{\mu}\frac{1}{p}\right.$$
$$\cdot\int_0^{\infty}\frac{\left[-\alpha\left(2\xi^2+\kappa^2\right)e^{-\alpha z}+2\alpha\left(\beta^2-\kappa^2\right)e^{-\beta z}\right]}{D}J_0(\xi r) \quad (87)$$
$$\left.\cdot J_1(a\xi)\,d\xi\right\}$$

Since

$$\lim_{a\longrightarrow 0}\left\{\frac{J_1(a\xi)}{a}\right\} = \frac{\xi}{2} \quad (88)$$

(86) and (87) yield the known [25] (80) and (81). With the aid of the Laplace inversion technique proposed in [25], (87) yields the wave propagation u_z on the soil surface for the pulse point load of (79):

$$u_z(r,0,t) = 0 \quad \text{for } \frac{c_2 t}{r} < \frac{1}{\sqrt{3}}$$

$$u_z(r,0,t) = \frac{P}{32\mu\pi r}\left\{6-\sqrt{\frac{3}{\left(c_2t/r\right)^2-0.25}}\right.$$
$$-\sqrt{\frac{3\sqrt{3}+5}{\left(3+\sqrt{3}\right)/4-\left(c_2t/r\right)^2}}$$
$$\left.+\sqrt{\frac{3\sqrt{3}-5}{\left(-3+\sqrt{3}\right)/4+\left(c_2t/r\right)^2}}\right\} \quad (89)$$
$$\text{for } \frac{1}{\sqrt{3}} < \frac{c_2t}{r} < 1$$

$$u_z(r,0,t) = \frac{P}{32\mu\pi r}\left\{6-\sqrt{\frac{3\sqrt{3}+5}{\left(3+\sqrt{3}\right)/4-\left(c_2t/r\right)^2}}\right\}$$
$$\text{for } 1 < \frac{c_2t}{r} < \frac{\sqrt{3+\sqrt{3}}}{2}$$

$$u_z(r,0,t) = \frac{3P}{8\mu\pi r} \quad \text{for } \frac{c_2t}{r} > \frac{\sqrt{3+\sqrt{3}}}{2}$$

For a unit load P=1, the displacement distributions at time instants t=0.0005s, 0.001s, 0.0015s, and 0.002s are demonstrated in Figures 3(a), 3(b), 3(c), and 3(d).

5. Conclusions and Discussion

In the present study, an exact solution of the vertical harmonic loading induced dynamic response in the elastic soil has been achieved. The present analytic solution can be utilized for solving the seabed response under vertical harmonic excitation of the wind turbine foundation in waves. The solution is based on integral transforms and stress functions. Verification to the solution has been conducted and a case study has been provided. The achieved solution for harmonic (with respect to time) pressure has been implemented for suddenly applied point load. The derived displacement functions for this transient point loading source are in full agreement with the existing [25] solution. For t=0.0005 s (Figure 3(a)) high values for u_z displacement take place in the vicinity of the point r=0 (loading source location). The displacement peak is surrounded by a valley ring which takes place in the area 0.987<r<0.222 m. For t=0.0015 s (Figure 3(b)) the peak is flattened and expanded in the area 0.0<r<0.208 m, and the valley ring is shallow. For t=0.0015 s (Figure 3(c)) the propagating peak is more flat and wide and is expanded in the area 0.0<r<0.388 m. For t=0.025 (Figure 3(d)) the plotted area 0.0<r<0.5 m is covered by the flat peak and no valley (in this area) is visible. The proposed method takes into account the inertial effects and does not require much computation power. Since the solution is analytic, the results are more accurate than numerical ones. The present work can be extended for solving viscoelastic porous media response under time-varying dynamic loads.

Appendix

A. Stress Components versus Displacements

See Figure 4.

$$\sigma_{xx} = (\lambda+2\mu)\left(\frac{\partial u_x}{\partial x}+\frac{\partial u_z}{\partial z}\right)-2\mu\frac{\partial u_z}{\partial z} \quad (A.1)$$

$$\sigma_{zz} = (\lambda+2\mu)\left(\frac{\partial u_x}{\partial x}+\frac{\partial u_z}{\partial z}\right)-2\mu\frac{\partial u_x}{\partial x} \quad (A.2)$$

$$\sigma_{yy} = \frac{\lambda}{2(\lambda+\mu)}\left(\sigma_{xx}+\sigma_{zz}\right) \quad (A.3)$$

$$\sigma_{xz} = \mu\left(\frac{\partial u_x}{\partial z}+\frac{\partial u_z}{\partial x}\right) \quad (A.4)$$

$$\sigma_{xz} = \mu\frac{\partial u_y}{\partial z} \quad (A.5)$$

$$\sigma_{xy} = 0 \quad (A.6)$$

B. Laplace Transform of the Displacement and Stress Components, Given by (12)-(20)

$$U_r = L\{u_r;t\longrightarrow p\} = \frac{\partial\Phi}{\partial r}+\frac{\partial^2\Psi}{\partial r\partial z} \quad (B.1)$$

$$U_\vartheta = L\{u_\vartheta;t\longrightarrow p\} = 0 \quad (B.2)$$

$$U_z = L\{u_z;t\longrightarrow p\} = \frac{\partial\Phi}{\partial z}+\frac{\partial^2\Psi}{\partial z^2}-\frac{p^2}{c_2^2}\Psi \quad (B.3)$$

$$S_{rr} = L\{\sigma_{rr};t\longrightarrow p\}$$
$$= \lambda\nabla^2\Phi+2\mu\left(\frac{\partial^2\Phi}{\partial r^2}+\frac{\partial^3\Psi}{\partial r^2\partial z}\right) \quad (B.4)$$

$$S_{\vartheta\vartheta} = L\{\sigma_{\vartheta\vartheta};t\longrightarrow p\} = \lambda\nabla^2\Phi+\frac{2\mu}{r}\left(\frac{\partial\Phi}{\partial r}+\frac{\partial^2\Psi}{\partial r\partial z}\right) \quad (B.5)$$

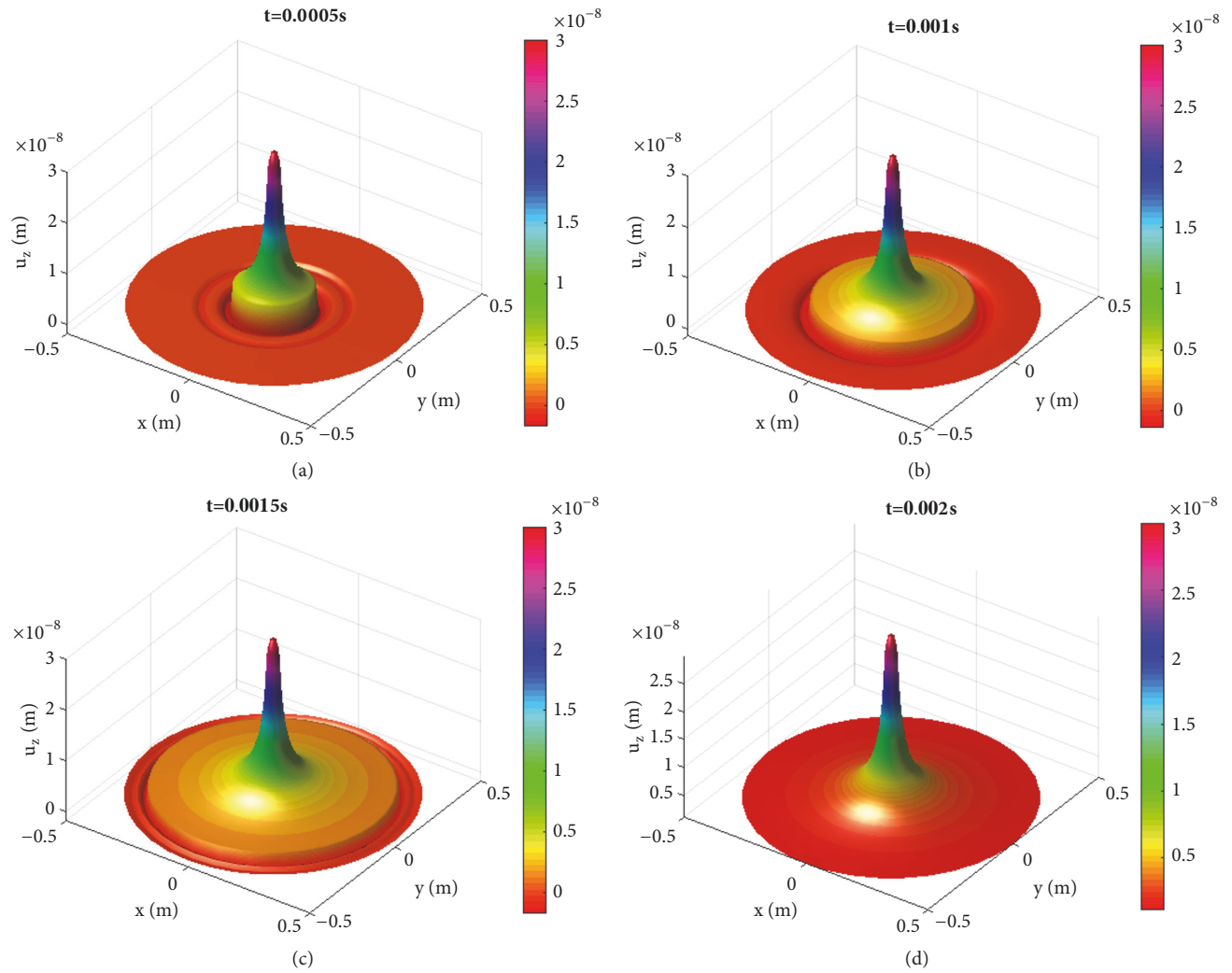

FIGURE 3: 3D displacement distribution of u_z due to transient point load for various time instants. Implementation of the proposed solution to transient point load shows full agreement with the existing solution in [25].

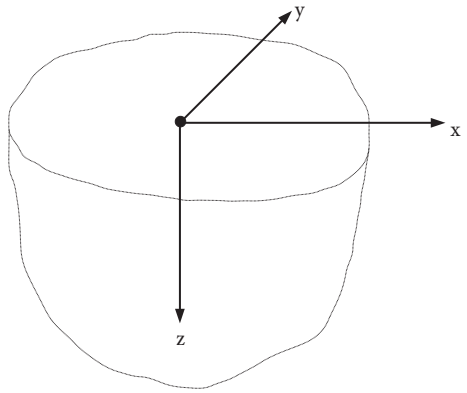

FIGURE 4

$$S_{zz} = L\{\sigma_{zz}; t \longrightarrow p\} = \lambda\nabla^2\Phi + 2\mu\frac{\partial}{\partial z}\left(\frac{\partial\Phi}{\partial z} + \frac{\partial^2\Psi}{\partial z^2} - \frac{p^2}{c_2^2}\Psi\right) \quad \text{(B.6)}$$

$$S_{rz} = L\{\sigma_{rz}; t \longrightarrow p\} = \mu\frac{\partial}{\partial r}\left(2\frac{\partial\Phi}{\partial z} + 2\frac{\partial^2\Psi}{\partial z^2} - \frac{p^2}{c_2^2}\Psi\right) \quad \text{(B.7)}$$

Data Availability

The data (i.e., equations and parameters that are used for reproducing the analytical solutions) used to support the findings of this study are included within the article.

Conflicts of Interest

The authors declare that they have no conflicts of interest.

References

[1] J. Ye, D. Jeng, R. Wang, and C. Zhu, "A 3-D semi-coupled numerical model for fluid-structures-seabed-interaction (FSSI-CAS 3D): Model and verification," *Journal of Fluids and Structures*, vol. 40, pp. 148–162, 2013.

[2] T. Sui, J. Zheng, C. Zhang et al., "Consolidation of unsaturated seabed around an inserted pile foundation and its effects on the wave-induced momentary liquefaction," *Ocean Engineering*, vol. 131, pp. 308–321, 2017.

[3] Z. Lin, D. Pokrajac, Y. Guo et al., "Investigation of nonlinear wave-induced seabed response around mono-pile foundation," *Coastal Engineering Journal*, vol. 121, pp. 197–211, 2017.

[4] Y. Li, M. C. Ong, and T. Tang, "Numerical analysis of wave-induced poro-elastic seabed response around a hexagonal gravity-based offshore foundation," *Coastal Engineering Journal*, vol. 136, pp. 81–95, 2018.

[5] Y. Li, T. Tang, and M. C. Ong, "3D Wave-Structure-Seabed Interaction Analysis of a Gravity-Based Wind Turbine Foundation," in *Proceedings of the ASME 2017 36th International Conference on Ocean, Offshore and Arctic Engineering*, pp. V009T10A009–V009T10A009, American Society of Mechanical Engineers, 2017.

[6] M. A. Biot, "General theory of three-dimensional consolidation," *Journal of Applied Physics*, vol. 12, no. 2, pp. 155–164, 1941.

[7] D. S. Jeng, *Offshore Geotechnics, Handbook of Ocean Engineering*, Dhanal Manhar and Xiros Nikolas, Eds., Springer, 2016.

[8] D. G. Pavlou, "Boundary element analysis of a plate on an elastic foundation loaded by a twisted annular rigid stamp," *Proceedings of the Institution of Mechanical Engineers, Part J: Journal of Engineering Tribology*, vol. 218, no. 6, pp. 549–555, 2004.

[9] D. Pavlou, "Green's Functions for Dissimilar or Homogeneous Materials Containing Interfacial Crack, Under Axisymmetric Singular Loading Sources," *International Journal of Computational Methods and Experimental Measurements*, vol. 5, no. 3, pp. 215–230, 2017.

[10] D. G. Pavlou, F. I. Mavrothanasis, C. Tsitouras, M. G. Pavlou, S. Avlonitis, and V. N. Vlachakis, "Stress concentration analysis of interfacial micro-structural cracks under internal singular loading sources," *Journal of Computational Methods in Sciences and Engineering*, vol. 10, no. 1-2, pp. 3–12, 2010.

[11] F. I. Mavrothanasis and D. G. Pavlou, "Green's function for KI determination of axisymmetric elastic solids containing external circular crack," *Engineering Fracture Mechanics*, vol. 75, no. 8, pp. 1891–1905, 2008.

[12] F. I. Mavrothanasis and D. G. Pavlou, "Mode-I stress intensity factor derivation by a suitable Green's function," *Engineering Analysis with Boundary Elements*, vol. 31, no. 2, pp. 184–190, 2007.

[13] D. G. Pavlou, "Green's function for a pre-stressed thin plate on an elastic foundation under axisymmetric loading," *Engineering Analysis with Boundary Elements*, vol. 29, no. 5, pp. 428–434, 2005.

[14] D. G. Pavlou, N. V. Vlachakis, and M. G. Pavlou, "An analytical solution of the annular plate on elastic foundation," *Structural Engineering and Mechanics*, vol. 20, no. 2, pp. 209–223, 2005.

[15] D. G. Pavlou, "Boundary-integral equation analysis of twisted internally cracked axisymmetric bimaterial elastic solids," *Computational Mechanics*, vol. 29, no. 3, pp. 254–264, 2002.

[16] D. G. Pavlou, "Green's function for the bimaterial elastic solid containing interface annular crack," *Engineering Analysis with Boundary Elements*, vol. 26, no. 10, pp. 845–853, 2002.

[17] D. G. Pavlou, "Dynamic response of an elastic medium containing crack," *Mechanics Research Communications*, vol. 69, pp. 27–33, 2015.

[18] D. G. Pavlou, "Dynamic response of a plate on elastic foundation under moving vertical and in-plane loads," *International Review of Mechanical Engineering*, vol. 9, no. 6, pp. 548–552, 2015.

[19] D. G. Pavlou, "Elastodynamic analysis of a thin layer bonded on a visco-elastic medium under combined in-plane and lateral pulse loads," *Mechanics Research Communications*, vol. 38, no. 8, pp. 546–552, 2011.

[20] D. G. Pavlou, "An exact solution for transient wave propagation in an infinite layer under dynamic torsion," *Mechanics Research Communications*, vol. 37, no. 4, pp. 372–376, 2010.

[21] W. Wu, G. Jiang, S. Huang, and C. J. Leo, "Vertical Dynamic Response of Pile Embedded in Layered Transversely Isotropic Soil," *Mathematical Problems in Engineering*, vol. 2014, Article ID 126916, 12 pages, 2014.

[22] Z. Zhang, J. Zhou, K. Wang, Q. Li, and K. Liu, "Dynamic Response of an Inhomogeneous Viscoelastic Pile in a Multilayered Soil to Transient Axial Loading," *Mathematical Problems in Engineering*, vol. 2015, Article ID 495253, 13 pages, 2015.

[23] Z. Wang, Y. Zhao, F. Li, and J. Jiang, "Extreme Dynamic Responses of MW-Level Wind Turbine Tower in the Strong Typhoon Considering Wind-Rain Loads," *Mathematical Problems in Engineering*, vol. 2013, Article ID 512530, 13 pages, 2013.

[24] Z. Wang, X. Liang, and G. Liu, "An Analytical Method for Evaluating the Dynamic Response of Plates Subjected to Underwater Shock Employing Mindlin Plate Theory and Laplace Transforms," *Mathematical Problems in Engineering*, vol. 2013, Article ID 803609, 11 pages, 2013.

[25] K. Graff, *Wave motion in elastic solids*, Dover, 1991.

[26] S. P. Timoshenko and J. N. Goodier, *Theory of Elasticity*, McGraw-Hill, New York, NY, USA, 2nd edition, 1970.

[27] M. Y. Antimirov, A. A. Kolyshkin, and R. Vaillancourt, *Applied integral transforms, CRM monograph series*, vol. 2, American Mathematical Society, 1993.

[28] A. H. D. Cheng, P. Sidauruk, and Y. Abousleiman, "Approximate inversion of the Laplace transform," *Mathematica Journal*, vol. 4, pp. 76–82, 1994.

[29] J. H. Knight and A. P. Raiche, "Transient electromagnetic calculations using the Gaver- Stehfest inverse Laplace transform method.," *Geophysics*, vol. 47, no. 1, pp. 47–50, 1982.

[30] https://www.wolfram.com/mathematica/.